ELSEVIER

Journal of Power Sources 58 (1996) 123–133

JOURNAL OF POWER SOURCES

Determination of an ageing factor for lead/acid batteries. 1. Kinetic aspects

C. Armenta-Deu, T. Donaire

Grupo de Energía Solar, Facultad de Físicas, Universidad Complutense, 28040 Madrid, Spain

Received 23 January 1995; revised 8 December 1995; accepted 11 December 1995

Abstract

The capacity of lead/acid batteries decreases with the number of cycles. This process is known as ageing. The reduction of capacity affects not only the operation time but also the performance of the accumulator and of the system attached to the battery. One of the main procedures affected by the battery ageing is the determination of the state-of-charge. In this paper, a parameter called 'ageing factor', f_a, which represents the reduction of the available energy in lead/acid batteries, is introduced. A method to calculate this factory and its incidence on battery performance has also been developed. The method is intended to predict 'ageing' effects on lead/acid batteries as a non-destructive method, as well as on-line battery operation. The method is based on the effective reduction in electrolyte specific gravity in a fully charged lead/acid battery computed from the change of the slope of the electrolyte density during charge with the number of cycles, and the subsequent reduction in discharge time. A correlation process between the reduction of the energy delivered by the electrochemical cell, the reduction of the discharge time, and the apparent change of the slope of electrolyte density has been developed, resulting in an analytical expression that may be used to compute the effective reduction in available energy in lead/acid batteries. The results of the experiments have proven the merit of the proposed system: the predicted values are in good agreement with experimental data, the associated error in the f_a estimation being lower than 9%, a result which has been considered acceptable to validate the proposed method.

Keywords: Lead/acid batteries; Ageing

1. Introduction

Lead/acid batteries may be discharged from very low rates (photovoltaic applications) to high peak discharges (UPS). The process of battery discharge does not, however, take account of the influence of cycling on the state-of-charge (SOC).

Ageing effects are barely mentioned in the literature and rarely quantified. Because of their evident influence on the battery performance, they must be taken into account when determining lead/acid battery characteristics, especially those concerning high rate discharges where the performance of the battery is more affected by ageing processes.

Cycling efficiency is one of the parameters most affected by ageing in lead/acid batteries. Usually, the SOC is estimated from the consideration of a 100% cycling efficiency, which in aged batteries is unreliable, especially after many cycles. The output voltage, a very common system to estimate the SOC in lead/acid batteries, is also affected by the ageing process with similar results to the cycling efficiency case. The traditional methods, therefore, may lead to an error in the determination of the SOC that can be as large as 30%. A correction factor to prevent ageing effects should be included to avoid problems derived from the erroneous determination of the available energy. This is of special importance in stand-alone systems which depend heavily on battery performance.

2. Ageing effects on battery performance

One of the main characteristics defining a lead/acid battery is its capacity when fully charged. The available cell capacity depends not only on the type of discharge but also on battery conditions. Charge or discharge involves different steps that can be placed in two main groups [1]: (i) ion transport to the double layer, and (ii) processes at the double layer and at the electrode wall, the latter group being most affected by battery ageing.

2.1. Kinetics of the electrode reactions

During the chemical reaction to transform chemical energy into electric current, sulfuric acid is used to generate lead sulfate and water. The process continues whilst acid is sup-

0378-7753/96/$15.00 © 1996 Elsevier Science S.A. All rights reserved
PII S0378-7753(96)02371-1

plied to the site of reaction and while lead or lead dioxide remains active. If either acid depletion or electrode passivation occurs the chemical reaction is interrupted and the battery fails.

The reverse process, the transformation of lead sulfate back to sulfuric acid, lead and lead dioxide, takes place during the recharge of the battery. Ruetschi [2] refers to the discharge process in the positive and the negative electrodes as a dissolution/precipitation mechanism, rather than a solid-state ion transport and film formation mechanism. Thus, during discharge of a lead electrode in sulfuric acid, lead sulfate crystals are formed. The same process occurs when lead dioxide is transformed into lead sulfate [3]. Growth of large $PbSO_4$ crystals during discharge, and of large Pb crystals during charge are commonly inhibited by the use of expanders as some authors have shown [4–9].

Expanders may be degraded during the battery life, thus allowing the formation of large crystals of lead sulfate. When large crystals of $PbSO_4$ are formed, the reverse reaction is inhibited because of the lower solubility of large $PbSO_4$ crystals. Also, $PbSO_4$ crystals become more stable when the battery remains uncharged for a long time. This process makes the battery age more rapidly than usual, a consequence of the non-reversible solution process of lead sulfate.

It is not clear what effect battery ageing has on the lead dioxide grain size. Lead sulfate crystals, when being transformed back to lead dioxide, forms crystals in two possible crystalline structures, α-PbO_2 and β-PbO_2, which have different discharge behaviours [10]. If α-PbO_2 is formed, rather than β-PbO_2, the battery will yield smaller discharge capacity [11]. This effect is attributed to the nucleation centres the α-PbO_2 apparently has, which helps the formation of $PbSO_4$ [12]. Therefore, if α-PbO_2 becomes the main component of the lead dioxide electrode, the battery capacity will be seriously reduced. How the ageing of a lead/acid cell influences the reverse process forming α-PbO_2 and β-PbO_2 is not yet known, but it is expected to have some type of influence on the process.

2.2. Influence of battery efficiency

The conversion of chemical to electric energy, and the reverse process, are carried out in electrochemical devices with efficiencies close to 100%, a theoretical value which is reduced by diverse factors affecting the chemical reactions. The overall efficiency of an electrochemical cell can be thermodynamically defined as the ratio of the free energy change to the enthalpy variation:

$$\eta_G = \Delta G / \Delta H \tag{1}$$

where ΔG represents the potential barrier of the electronic change at the electrode surface, and ΔH the change of enthalpy in the system during the reaction, provided that it takes place at constant pressure.

The change of the free energy, ΔG, can be expressed in electrical terms from:

$$\Delta G = nFV_e \tag{2}$$

where n is the electronic change, F the Faraday number, and V_e the cell voltage at equilibrium.

The overall efficiency is, on the other hand, modified by changes in the local potential ϕ_s when electron transfer occurs. The local voltage is affected by the activation and concentration overpotential, η_a and η_c, respectively.

Because the contribution of the potential due to the dipole action at both electrodes, $\Delta\epsilon$, is much lower than the external potential $\Delta\Phi$, we can neglect the dipole contribution, resulting in:

$$V = \Delta\phi = \Delta\Phi \tag{3}$$

and considering the contribution of the activation and concentration overpotentials:

$$V = V_e - \eta_a - \eta_c = V - \eta \tag{4}$$

which, taking into account voltage and faradaic efficiencies, leads to:

$$\eta_G = (nFV/\Delta H)/(ItE/\Delta m) \tag{5}$$

Battery ageing affects both voltage and charge efficiency. Nevertheless, we will restrict our present study to the influence of ageing on mass transfer, the effects on enthalpy change and on overpotential being the subject of future works.

2.3. Density slope

Charge and discharge processes in a lead/acid cell follow the reversible reaction:

$$Pb + PbO_2 + 2H_2SO_4 \leftrightarrow 2PbSO_4 + 2H_2O \tag{6}$$

with the reaction displaced to the right for the discharge.

Because of the irreversibility in the charge/discharge reactions, the sulfuric acid is sometimes transformed into large $PbSO_4$ crystals which cannot be recovered back to H_2SO_4. Thus, the SG of aged lead/acid batteries after the charge half-cycle is lower than in the new ones [1]. This process occurs, even though we overcharge the cell to homogenize the electrolyte or we use one of the alternative methods [13–15] (see Fig. 1(a)). The lower value of the H_2SO_4 solution indicates that part of the $PbSO_4$ has not been transformed back into active material, Pb and PbO_2. Two phenomena are implied in this process, one purely kinetic, the other affecting the plate structure [2].

[1] It is assumed that electrolyte SG is not manually altered by refilling the cell cup with pure sulfuric acid or concentrated electrolyte which would disturb the proposed method. If evaporation process occurs because of excessive overcharge, only water should be added to the cell, the only component that evaporates.

[2] When slow battery charge and discharge are applied, e.g. photovoltaic set-ups, large $PbSO_4$ crystals are formed. At the positive battery plates, oxidation of $PbSO_4$ to PbO_2 proceeds usually through metasomatic processes. Oxidation starts at the surface and advances into the interior of the $PbSO_4$ crystal. This is a slow process and a considerable part of the crystal interior remains unoxidized [1], which in its turn causes the plate capacity to decrease.

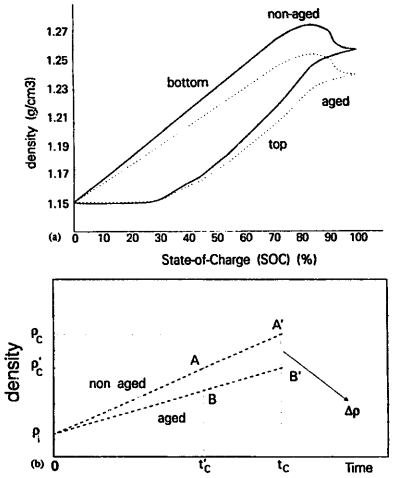

Fig. 1. (a) Density profiles of aged and non-aged lead/acid batteries during charge. (b) 'Apparent' density profiles of aged and non-aged lead/acid batteries during charge.

The extremely high concentration gradient between top and bottom of the cell, and its dependence on charge conditions makes the charge process have different density profiles, therefore, the density profile is worthless.

To solve the problem, we consider the charge process conducted under homogeneous conditions, where, there is no concentration gradient between top and bottom of the cell. This results in an apparent density profile (see Fig. 1(b)) that summarizes the full process of charge. It is clear that as the battery ages the slope of the process of charge will decline. The effect of battery ageing can then be computed from the ratio of the two slopes, the one for the non-aged battery and the one for the aged cell.

The discharge process, however, is of no use because, according to Faraday's law, the slope of the discharge depends on the charge drawn from the battery. If the same conditions are applied to both, non-aged and aged batteries, the SG slope will be the same for both cells (see Fig. 2) [3].

3. Determination of the ageing factor

We have already mentioned that the SG of a fully charged aged battery is lower than that corresponding to a non-aged one in the same conditions. From the observation of Fig. 1(b), we notice the difference between the respective SG for the two cells, ρ_{Cn} for the non-aged battery, and ρ_{Ca} for the aged one. The difference:

$$\Delta\rho = \rho_{Cn} - \rho_{Ca} \tag{7}$$

gives us an indication of how the battery has aged.

Battery ageing has been traditionally associated with the loss of the delivered energy; therefore, the ageing factor, f_a, can be defined as:

$$f_a = Q_{loss}/Q_{total} \tag{8}$$

from where,

$$f_a = 1 - Q_a/Q_n \tag{9}$$

where Q_a and Q_n are the delivered energy of the aged and non-aged batteries, respectively.

It is well known that energy delivered from a lead/acid cell is directly related to the change of the SG in the cell; therefore, we can use the expression:

$$\rho_i = \rho_C + m_D t_i \tag{10}$$

with t_i being the current time from the beginning of discharge, and m_D the discharge slope, given by:

$$m_D = \Delta\rho/t_D = (\rho_C - \rho_D)/t_D \tag{11}$$

where ρ_C and ρ_D are the SG of the fully charged and fully discharged battery, and t_D is the discharge time.

Eq. (10) is valid for all types of battery, even those using mechanical methods to homogenize the electrolyte during charge or discharge [16].

The minimum SG of a lead/acid cell in a discharge process depends on the type of discharge, and more precisely, on the current extracted from the battery. However, if we compare the behaviour of a non-aged and an aged lead/acid cell for the same operation conditions, the minimum SG at the end of the discharge will be the same for both. This situation has been represented in Fig. 3, where a typical discharge process in two lead/acid batteries, aged and non-aged, has been drawn. The non-aged battery starts at a SG of ρ_{Cn} and ends at ρ_D, the established minimum SG of the cell for the current

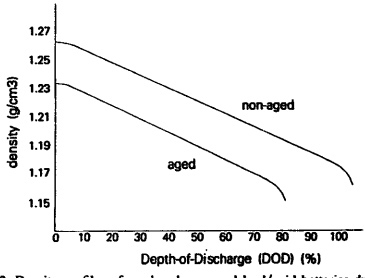

Fig. 2. Density profiles of aged and non-aged lead/acid batteries during discharge.

[3] According to Faraday's law, discharge density curves should be linear. Deviations from this rule at the beginning may be due to the presence of a certain amount of H_2 and O_2 produced during charge. At the end of the discharge, the non-homogeneous stratification of the electrolyte in the active block of the cell produces a sudden change in the density slope.

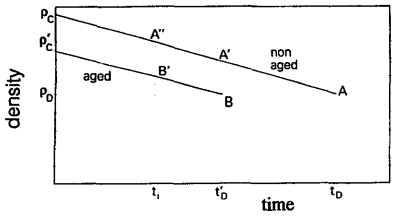

Fig. 3. Discharge time for aged and non-aged lead/acid batteries.

discharge process. The aged battery, however, starts at ρ_{Ca} and ends at the same minimum SG, ρ_D. Due to the completion of the Faraday's law, the discharge slope is the same for both cells, therefore, the aged battery fails earlier (t'_D) than the non-aged one (t_D).

Making use of Eq. (10) for both, aged and non-aged batteries, during discharge:

$$\rho_i = \rho_{Cn} + m_D y t_i \tag{12}$$

and

$$\rho'_i = \rho_{Ca} + m_D t_i = \rho_{Cn} - \Delta\rho + m_D t_i \tag{13}$$

where ρ_i and ρ'_i the current SG for the non-aged and aged cell, respectively.

From these Eqs. we can determine the remaining time for both cells:

$$t_r = t_D - (\rho_{Cn} - \rho_i)/m_D = t_D - t_i \tag{14}$$

and

$$t'_r = t'_D - (\rho_{Ca} - \rho_i)/m_D = t'_D - t_i \tag{15}$$

from which

$$t_r - t'_r = t_D - t'_D = \Delta\rho/m_D = (\rho_{Cn} - \rho_{Ca})/m_D \tag{16}$$

The densities or specific gravities at the end of charge can be determined easily through accurate measurements, but this does involve electrolyte homogenization. This homogenization process is usually attained by gassing for some hours after the charge process has finished. The inherent problems associated with the gassing method are well known and this will not be emphasized here. We will just mention the cost of the extra energy, the waste of evaporated water and the damage caused to the plates because of the high voltage used in the process. In order to homogenize the electrolyte the density at the end of the charge may be obtained from the charging time and the density slope, if no alternative method is available.

In the charge process for a non-aged battery (see Fig. 1(b)), the SG of the cell at the end of the charge may be obtained from:

$$\rho_{Cn} = \rho_0 + m_{Cn} t_C \tag{17}$$

where ρ_0 is the initial SG.

In the same way, for the aged battery,

$$\rho_{Ca} = \rho_0 + m_{Ca} t_C \tag{18}$$

From Eqs. (17) and (18) can be obtained:

$$\Delta\rho = \rho_{Cn} - \rho_{Ca} = (m_{Cn} - m_{Ca}) t_C \tag{19}$$

and using Eq. (9), and the relation between cell capacity and SG, results in:

$$f_a = 1 - m_{Ca}/m_{Cn} \tag{20}$$

Combining Eqs. (16), (19) and (20),

$$t_D - t'_D = (m_{Cn}/m_D) t_C f_a \tag{21}$$

Remembering the discharge process follows Faraday's law, we can now define the reduction of the available energy as:

$$F = Q_u/Q_n = m_D t'_D/m_D t_D = t'_D/t_D \tag{22}$$

and from Eq. (21),

$$F = 1 - f_a = m_{Ca}/m_{Cn} \tag{23}$$

where the fact that for a non-aged battery the charge/discharge cycle is a fully reversible process with no energy losses has been considered, therefore, $Q_n = Q_D$, and that $Q_n = m_{Cn} t_C$, $Q_D = m_D t_D$.

Eq. (23) provides a useful way to compute the reduction of the delivered energy in an aged battery from the ratio of the charge slope of the aged to the one of the non-aged battery.

As the density slope varies with charge and discharge conditions, the ageing factor should be characterized for every case, thus having:

$$f_a = f_a(C, I_C, I_D) \tag{24}$$

The influence of the capacity on the ageing factor may be overcome if one deals with cells of the same capacity; otherwise, a characterization process for every element is required.

The characterization of all possible discharge rates would require a massive effort; fortunately, many battery applications follow the same patterns, fixed discharge rates at C_{10}, C_{20}, and occasionally C_5, for aotomotive and traction batteries, and at C_{100} for photovoltaic (PV) applications. This reduces the ageing factor estimation to two or three cases representing the majority of lead/acid battery uses.

A similar consideration could be taken into account for the charge process; unfortunately, in some systems, especially PVs, the charge current is not constant and the process to characterize the ageing factor becomes more complex.

3.1. Determination of the density profile during charge

Two different methods are proposed for the determination of the ageing factor: (i) determination of the density slope at the process of charge, or (ii) use of a reference cell to compute changes in density [17].

Every charge process is represented by a single point, this point being the average slope of density variation from start-

ing to end during charge, considering the process to be linear. The assumption of a linear evolution of electrolyte density in a charge process in lead/acid cells, introduces a non-significant error that can be neglected if charge rate is low ($I_C < C_5$).

Measurements of the density and of the density profile during charge supposes that samples are extracted at regular intervals from the cell, and the density determined by gravimetric methods or by ultrasonic meters. A high precision is obtained with the use of this methodology, 0.1 mg cm^{-3}, but requires continuous extractions. An alternative method has been developed in our laboratory using a reference cell linked to a pumping system [17], which provides a reference voltage directly related to the change of cell density. From this voltage the determination of the density slope is easy to obtain.

The different profile showed by the electrolyte density during charge in the top and bottom zones of the lead/acid cell introduces some error if not taken into account, so the point from which the sample is extracted is critical. The problem can be avoided with the use of a system to homogenize the electrolyte. The method is more precise, but not applicable to all lead/acid batteries, assuming that most lead/acid cells do not include agitation or recirculation systems.

Top or bottom density profile can be corrected by a factor to fit the imaginary process of a constant density profile charge in a lead/acid battery. However, the density at the top of the cell only starts to rise after 30% of the full charge is attained, and changes suddenly when the battery reaches the 80% of the full charge (see Fig. 1(a)). This fact limits the field of application of the proposed method to a range of 30–80% of the SOC if density is measured at the top. The bottom profile shows a more regular behaviour, with almost constant slope from the very beginning (0%) of the charge until the very late stages of charge (80%). The constancy in the slope of the density for almost all the charge range makes the density measurement at the bottom more reliable and useful for practical purposes. Therefore, the method must be restricted to density measurements at the bottom of the cell, if no electrolyte circulation or mechanical agitation is used, which for charge processes at low current can be considered representative of the charging process.

3.2. Cell characterization

In lead/acid cells with mechanical agitation or electrolyte circulation the slope of the density during charge can be directly obtained from the density measurements. In cells with density gradient a prior characterization of the cell is necessary. For that, a new cell of the same characteristics of those that are going to be used, must be submitted to a full process of charge measuring density at the bottom from which the slope of the density is obtained and compared with that of the process of a constant density profile (see Fig. 1(b)). The ratio between the two slopes give us the correction factor for the characterization of the cell. This correction factor should be one of the technical data included by the manufacturer to the user.

3.3. Experimental methodology

Experiments have been carried out in lead/acid cells of 240 Ah and 150 Ah, both at C_{10} charge rates. Tested cells were previously characterized at zero-ageing state, determining capacity at different discharge rates, drawing charge and discharge curves, and establishing the density variation curve versus delivered energy. The density variation curve was correlated to a straight line with a correlation factor higher than 95%.

Tested elements were submitted to a process of accelerated ageing through processes of deep cycling. The ageing process was different for every element. Ten different cells of 240 Ah lead/acid batteries, and eight of 150 Ah were used.

Discharge tests were carried out from C_5 to C_{100} discharge rate, referred to the non-aged state. Charge processes were conducted under various conditions simulating PV and automotive and traction duty cycles. Low discharge current for PV duty varied from C_{20} to C_{100} while high discharge current for automotive and traction batteries moved from C_5 to C_{10}.

The density slope for charge or discharge processes was obtained from the expression:

$$m_i = [\rho(t_i) - \rho(t_0)]/(t_i - t_0) = \Delta\rho/\Delta t \quad (25)$$

for agitated batteries, and

$$m'_i = f_{ch} m_i \quad (26)$$

for conventional ones, f_{ch} being the characterization factor for density slope correction.

Density slope values of the charge process for aged and non-aged cells were then correlated to capacity according to:

$$m = aQ + b \quad (27)$$

where Q and m are the full capacity of the battery, and the density slope, respectively, and a and b are the correlation coefficients.

The ageing factor has been computed from Eqs. (9) and (20) and plotted against the density slope at the charge process for the aged battery (Fig. 4). The dotted line represents the real ageing factor (f_a, Eq. (9)), while the continuous line

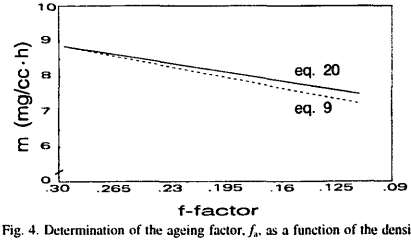

Fig. 4. Determination of the ageing factor, f_a, as a function of the density slope in aged lead/acid batteries during charge.

is the estimated factor from the charge slopes (f_a, Eq. (20)). The slope of the straight continuous line is the reverse of the slope corresponding to the charge process of a non-aged battery, a process that can be considered ideal because of the reversibility of the reactions taking place in the cell. The intersection with the x-axis represents the deviation from the predicted value for a non-aged battery.

The graphical representation provides a quick way to visualize the ageing factor from a slope value, and it is easy to use, especially if one deals with more than one type of cell. Nevertheless, the graphical method has the drawback of needing a family of curves, one for every charge process. To solve this problem we can deduce a relation between all correlation coefficients, a and b, corresponding to different charge conditions. In such a case, one would have:

$$m_{Ca} = a(I_C)Q_a + b(I_C) \tag{28}$$

or

$$Q_a = A(I_C)m_{Ca} + B(I_C) \tag{29}$$

with $A(I_C) = 1/a(I_C)$ and $B(I_C) = -[b(I_C)/a(I_C)]$.

The functions $A(I_C)$ and $B(I_C)$ permit the user to move from curve to curve, even to those that correspond to non-standard uses. The method, thus, requires a single analytical expression for the ageing factor, and complementary functions to determine the dependence of correlation parameters on charge conditions.

3.4. Experimental results

Fig. 5(a) and (b) represents the ageing factor versus density slope for the 240 Ah and 150 Ah lead/acid batteries, respectively. Every test has been represented by a point in the graph.

The spread of experimental data with the increase in density slope can be explained by the evolution of the structure of the two active masses or some irregular behaviour of the aged battery, with some type of unforeseen performance, probably due to secondary chemical reactions.

The density slope decreases as the battery ages, according to theoretical analysis. The slope, however, is not constant for different charge conditions and requires the definition of an analytical dependence of correlation parameters a and b on current.

From the linearity showed in the experiments between f_a and m_{Ca} follows:

$$f_a = A_0 m_{Ca} + B_0 \tag{30}$$

or

$$m_{Ca} = a_0 f_a + b_0 \tag{31}$$

where

$$A_0 = 1/a_0 \tag{32}$$

and

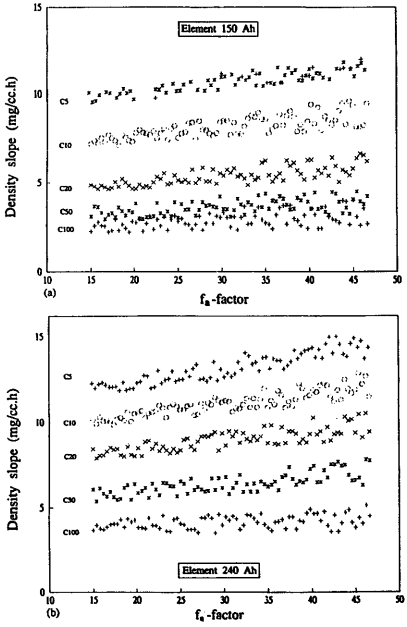

Fig. 5. (a) Ageing factor, f_a, vs. density slope, m_{Ca}, for a 150 Ah lead/acid battery. (b) Ageing factor, f_a, vs. density slope, m_{Ca}, for a 240 Ah lead/acid battery.

$$B_0 = -(b_0/a_0) \tag{33}$$

from which, Eq. (29) can be arranged as:

$$f_a = a_1 Q_a + b_1 \tag{34}$$

where

$$a_1 = \frac{1}{a_0 A(I_C)} \tag{35}$$

and

$$b_1 = -\left[\frac{b_0}{a_0} + \frac{B(I_C)}{a_0 a(I_C)}\right] \tag{36}$$

Eq. (34) shows an alternative way to determine the ageing factor when the charge supplied to the aged battery is known.

A linearity test has been run to check the validity of Eqs. (30) and (31), the result of which is shown in Table 1. The decreasing of the RMS coefficient with discharge rate has been attributed to the irreversibility that happens in the electrochemical reactions at the double layer when the cell is being charged or discharged; the more rapid the charge (or discharge), the more irreversible the reactions become, therefore the aged battery behaviour is more predictable.

Table 1
Linearity factor for the relation m_{C_a} vs. f_a

Capacity (Ah)	Process	RMS
150	C_5	0.961
150	C_{10}	0.959
150	C_{20}	0.943
150	C_{50}	0.921
150	C_{100}	0.890
240	C_5	0.876
240	C_{10}	0.869
240	C_{20}	0.852
240	C_{50}	0.825
240	C_{100}	0.791

Table 2
Correlation coefficients for the relation m_{C_a} vs. f_a

Capacity (Ah)	Process	a_0	b_0
150	C_5	−0.01137	9.8895
150	C_{10}	−0.02157	7.5924
150	C_{20}	−0.04277	5.1199
150	C_{50}	−0.08441	3.5158
150	C_{100}	−0.16352	2.3521
240	C_5	−0.00602	13.2149
240	C_{10}	−0.01160	10.8923
240	C_{20}	−0.02267	6.8899
240	C_{50}	−0.04385	4.1105
240	C_{100}	−0.08364	3.0125

Coefficients a_0 and b_0 in Eq. (31) have been deduced from the numerical analysis from results of Fig. 5(a) and (b). Once these coefficients have been obtained, the ageing factor f_a can be easily determined. Numerical results of a_0 and b_0 have been included in Table 2. To determine both parameters for every case, we have applied a linear correlation to the results included in Table 2. Thus:

$$a_0(C_x) = \alpha_1 x + \beta_1 \quad (37)$$

$$b_0(C_x) = \alpha_2 x + \beta_2 \quad (38)$$

where C_x is the type of process, and x the charge or discharge time.

The coefficients of this correlation have been presented in Table 3.

The two coefficients a_0 and b_0 permit the determination of the ageing factor with a minimum amount of calculation. The problem is, however, based on the necessity to define a couple of parameters (a_0, b_0) for every battery and every process. This makes the method unwieldy, requiring an enormous amount of data, and computerization when different charge or discharge rates are used during the process. The problem can be solved, if we can derive an analytical expression, relating general coefficients of a reference battery [4] for a standard process [5], to the ones corresponding to the tested battery at the fixed charge or discharge rate.

Based on this idea, a relation between linear coefficients of 150 Ah and 240 Ah cells, for C_5 to C_{100}, has been deduced. The relation links coefficients of different types of discharge for every battery. The parameters that represent this relation have been previously defined, as follows:

$$A(I_C) = A_x = a_0(C_x)/a_0(C_{10}) \quad (39)$$

and

$$B(I_C) = B_x = b_0(C_x)/b_0(C_{10}) \quad (40)$$

where C_x is the rate of the process (C_5 to C_{100}), the C_{10} is the reference charge/discharge cycle.

Using data from Table 2 we obtain the parameter A_x and B_x for all the tested rates (Table 4).

Coefficients A_x and B_x can be linearly correlated to obtain them from a simple relation for every type of process. The values so obtained are:

$$A_x = \alpha_a x + \beta_a \quad (41)$$

and

$$B_x = \alpha x^{\beta} \quad (42)$$

[4] Any type of battery may act as a reference battery.
[5] C_{10} charge and discharge rate.

Table 3
Correlation of coefficients a_0 and b_0 (Table 2) for lead/acid batteries of 150 Ah and 240 Ah

Process	a_0: 150	a_0: 240	b_0: 150	b_0: 240
C_5	−0.01137	−0.00602	9.8895	13.2149
C_{10}	−0.02157	−0.01160	7.5924	10.8923
C_{20}	−0.04277	−0.02267	5.1199	6.8899
C_{50}	−0.08441	−0.04385	3.5158	4.1105
C_{100}	−0.16352	−0.08364	2.3521	3.0125

a) *Regression coefficients*, b_0: 150		b) *Regression coefficients*, b_0: 240	
Constant	21.900	Constant	32.563
Coefficient determination (r^2)	0.996	Coeffifient determination (r^2)	0.990
Coefficient X	−0.478	Coefficient X	−0.519
c) *Regression coefficients*, a_0: 150		d) *Regression coefficients*, a_0: 240	
Constant	−0.0065	Constant	−0.00393
Coefficient determination (r^2)	0.997838	Coefficient determination (r^2)	0.997144
Coefficient X	0.00157	Coefficient X	−0.0008

Data concerning the correlation of A_x and B_x as a function of C_x are presented in Table 5.

Remembering one is using the C_{10} as the standard process, and combining Eqs. (30), (32) and (33), one obtains the final expression for the f_a factor for all type of battery processes:

$$f_a=\left[\frac{1}{A_x a_0(C_{10})}\right]m_{Ca}-\left[\frac{b_0(C_{10})}{a_0(C_{10})}\right]\left[\frac{B_x}{A_x}\right] \quad (43)$$

3.5. Results

The slight deviations from the predicted values have been attributed to changes in the efficiency of the charge/discharge cycle, which varies with cell ageing as authors have demonstrated [18].

The reader can notice the very low values of the density slope, tenths of milligrams per cubic centimeter per hour; therefore, a very precise detection meter is required. It has already been mentioned that gravimetric or ultrasonic devices give a maximum precision of 0.1 mg cm^{-3}; this precision is, in some cases, insufficient and leads the user to relative high errors in the determination of the ageing factor. The solution is to use a reference cell [19] which improves the precision, usually by a factor of ten, reducing the error in the f_a determination. Thus, if high precision is required, the use of a reference cell becomes mandatory.

Relatively high values of battery ageing (40%) have been accepted, in contrast with convention (maximum depth of discharge of 20%). The reason to extend the ageing limit is to apply lead/acid batteries to especial working conditions, such as PV systems, which operate under very low currents ($I_D=C_{100}$), making the voltage decrease quite slowly during operation, and enlarging discharge time and low cell capacity acceptance.

3.6. Validation of the generalization of f calculation

Eq. (43) provides a quick and easy way to compute the ageing factor for any type of discharge. However, the method must be validated, prior to its general use, for the expected range to which lead/acid batteries will be applied. Conventional assignments consider a lead/acid battery to be dead if delivered energy is lower than 80% of the maximum for the same discharge rate. More flexible conventions accept a limit of 30% of degradation in battery lifetime before rejecting the element. From these considerations, we have developed an analytical expression which yields the estimated error in the f_a determination, giving us the limit in which f_a is being calculated within an acceptable error.

Table 4
Correlation coefficients for the relation m_{Ca} vs. f_a

Capacity (Ah)	Process	A	B
150	C_5	0.527	1.303
150	C_{10}	1.000	1.000
150	C_{20}	1.983	0.674
150	C_{50}	3.913	0.463
150	C_{100}	7.581	0.310
240	C_5	0.519	1.213
240	C_{10}	1.000	1.000
240	C_{20}	1.954	0.633
240	C_{50}	3.780	0.377
240	C_{100}	7.210	0.277

From Eq. (43) one may deduce:

$$\Delta f_a=A_0\,\Delta m+\left[\frac{m_{Ca}}{(a_0A_x)^2}\right][A_x\,\Delta a_0+a_0\,\Delta A_x]+\left[\frac{1}{a_0}\right][a_0\,\Delta b_0+b_0\,\Delta a_0]\left[\frac{B_x}{A_x}\right]+\frac{B_0A_x\,\Delta B_x+B_x\,\Delta A_x}{a_0\quad A_x^2} \quad (44)$$

where Δx is the absolute error in calculating the magnitude x.

To be sure about the validity of the method, a further correlation has been made between the density slope variation and the f_a factor itself, establishing the detection limit of f_a as 0.40, 20% higher than the conventional criteria for lead/acid battery lifetime. The results of that correlation have been included in Table 6.

3.7. Error analysis

The ageing factor may be considered acceptable if the error associated with its determination remains between certain limits. For this purpose an error expression, from the analytical formula of the f_a factor has been deduced.

Using statistical analysis we obtain,

$$\epsilon_f=2(\Delta m/m_{Ca})+\{[\Delta m+c(\sigma_a'+\sigma_b')]/(m_{Ca}+c)\} \quad (45)$$

where ϵ_f is the relative error associated to f_a, Δm the absolute error in the slope calculation, σ_a' and σ_b' the relative standard errors of the correlation coefficients a and b (Eq. (27)), and $c=a/b$.

The relative standard errors σ_a' and σ_b' are given by:

$$\sigma_a'=\sigma_a/a$$

and

$$\sigma_b'=\sigma_b/b \quad (46)$$

where

$$\sigma_a=\sigma_0/[\Sigma m_i^2-(\Sigma m_i)^2/n]^{1/2} \quad (47)$$

$$\sigma_b=\sigma_0/[\Sigma m_i^2/n\{\Sigma m_i^2-(\Sigma m_i)^2/n\}]^{1/2} \quad (48)$$

being

$$\sigma_0=[\Sigma(f_i-f_a)^2/(n-2)]^{1/2} \quad (49)$$

Table 5
Linear correlation for the $A(x)$ and $B(x)$ coefficients

Battery capacity (Ah)	Process	Discharge time (h)	$A(x)$	$B(x)$
150	C5	5	0.527	1.303
150	C10	10	1.000	1.000
150	C20	20	1.983	0.674
150	C50	50	3.913	0.463
150	C100	100	7.581	0.310
240	C5	5	0.519	1.213
240	C10	10	1.000	1.000
240	C20	20	1.954	0.633
240	C50	50	3.780	0.377
240	C100	100	7.210	0.277
a) *Regression coefficients*, $A(x)$: 150		b) *Regression coefficients*, $B(x)$: 150		
Constant	0.301	Constant		2.893
Coefficient determination (r^2)	0.998	Coefficient determination (r^2)		0.996
Coefficient X	0.073	Coefficient X		−0.479
c) *Regression coefficients*, $A(x)$: 240		d) *Regression coefficients*, $B(x)$: 240		
Constant	0.339	Constant		2.987
Coefficient determination (r^2)	0.997	Coefficient determination (r^2)		0.990
Coefficient X	0.069	Coefficient X		−0.518

Table 6
Maximal allowance in the determination of the f factor

Capacity (Ah)	Process	f_a'
150	C_5	40.65
150	C_{10}	41.16
150	C_{20}	42.44
150	C_{50}	45.11
150	C_{100}	48.82
240	C_5	40.95
240	C_{10}	41.54
240	C_{20}	42.04
240	C_{50}	44.92
240	C_{100}	46.79

Two cases can be considered from the statistical point of view, low and intermediate errors in σ_a and σ_b. The first case corresponds to almost null data scattering, being:

$$c \gg \Delta m; \quad c \gg m_{Cn} \tag{50}$$

In such a case, the global f_a error adopts the form:

$$\epsilon_f = 2(\Delta m/m_{Ca}) + \sigma_a' + \sigma_b' \tag{51}$$

If data scattering becomes greater (intermediate standard error), Eq. (51) is no longer useful, because of lack of compliance with Eq. (50), and we have to go back to Eq. (45) to estimate ϵ_f.

The f_a error may be improved if we use a reference electrode to determine the density. From the expression which links reference voltage and density [17] one obtains:

$$f_a = (1/\Delta t)(k_1 + k_2 \Delta V_r)/[(k_1 + k_2 V_r) + c] \tag{52}$$

where Δm has been substituted by the reference voltage V_r, Δt is the time interval, and k_1 and k_2 are the correlation coefficients.

From Eq. (52) one may deduce:

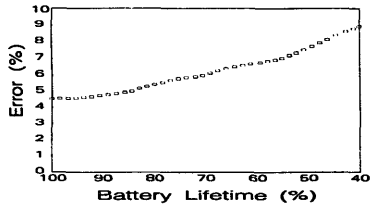

Fig. 6. Estimation of the relative error in the determination of the ageing factor for lead/acid batteries.

$$\epsilon_f = [\blacktriangledown(\Delta t)/\Delta t] + \{[(\sigma_{k_1} + \sigma_{k_2}\Delta V_r + k_2 \blacktriangledown(\Delta V_r)]/(k_1 + k_2 V_r)\} + \{[(\sigma_{k_1} + k_2 \Delta V_r + V_r \sigma_{k_2}) + c(\sigma_{k_1}' + \sigma_{k_2}')]/(k_1 + k_2 V_r + c)\} \tag{53}$$

The use of a reference voltage to determine the f_a factor has the advantage to avoid the extraction of samples from the cell; it also makes the error in the determination of the ageing factor lower as can be seen in Fig. 6.

3.8. Application of the f factor

The determination of the SOC of a battery during operation is essential for a correct prediction of the cutoff point and for a reliable behaviour of the battery, on which depend most of the PV components of a PV solar unit. SOC methods based on electrical measurements or on electrolyte density tests have been developed for non-aged batteries. Therefore, as a battery ages the cell behaviour departs from ideal, and the predicted SOC using these methods is no longer valid. The use of the correct f_a factor for aged batteries easily solves the problem, because it takes into account the degradation of the battery. As this factor has been deduced from kinetic consid-

erations, it best applies to methods that use electrolyte density to predict the SOC of the battery [6].

4. Conclusions

The paper presents a simple method to compute the ageing factor in lead/acid batteries. The knowledge of the f_a factor can be applied to many battery characteristics such as the reduction of cell capacity, prediction of the SOC, average battery lifetime, changes in performance, etc. All of them will permit the user to predict the battery behaviour with a low error.

The method provides users and system designers utilizing lead/acid batteries with a tool to continuously control the system regarding battery ageing. Therefore, the equipment attached to the battery will never be shut off because of a premature collapse of the battery.

Two different solutions for the computation of the ageing factor have been proposed in the work. The first is less accurate but simplest to use, because the only requirement is changes in density, obtained either from extraction of samples or from a reference voltage. The second method is more complicated and requires a characterization prior to operation; however, it gives a higher precision and is recommended when good accuracy is needed.

Battery ageing has been revealed as an important factor to be considered in the general design of a system linked to a battery. The ageing limit for a lead/acid battery is, in most applications, established at the 80% of the overall capacity. This limit is, in the authors' opinion, too conservative, and should be reviewed for some applications such as PV arrays operating at low rates.

The estimation of the f_a factor has been found to be influenced by some data scatter which depends on ageing. This data scatter has been attributed to the evolution of the structure of the two active masses or some irregular behaviour of the aged battery, probably due to secondary chemical reactions.

A method to compute the f_a factor for all kind of batteries processes has been validated for the range $0 < f < 0.40$, 10% deeper than the maximum conventionally accepted range of battery lifetime ($f_a^{\max} = 0.3$).

5. List of symbols

A, B, A_0, B_0	correlation coefficients
a, b, a_0, b_0	correlation coefficients
C	cell capacity
C_x	cell capacity at x-rate (in h)
E	electrochemical equivalent
F	Faraday number
f_{ch}	characterization factor for non-agitated batteries
I, I_D	discharge current
I_C	charge current
Q, Q_n	overall capacity of the non-aged cell
Q_1, Q_a	capacity of the aged cell
Q_{total}	overall cell capacity
Q_{loss}	loss of capacity in the aged battery
V	cell voltage
V_e	cell voltage at the equilibrium
V_r	reference voltage
f_a	ageing factor
k_1, k_2	correlation coefficients for the f_a determination using reference voltage measurements
m, m_i	density variation slope
m_{Cn}	density variation slope for the non-aged battery
m_{Ca}	density variation slope for the aged battery
m_i'	density variation slope for the non-agitated batteries
m_D	density variation slope during discharge process
n	electronic change; number of samples
t	time
t_D, t_D'	discharge time
t_i	current time
t_r, t_r'	remaining discharge time

Greek letters

ϵ_f	error in f determination
ρ_0	initial density
ρ_C	density of a fully charged battery
ρ_D	density of a fully discharged battery
ρ_i'	density of an aged battery
ρ_i	density of a non-aged battery
ρ_{Ca}	density of the aged battery when fully charged
ρ_{Cn}	density of the non-aged battery when fully charged
σ_a, σ_b	standard errors of a and b, respectively
σ_0	standard error of f
σ_{k1}, σ_{k1}	standard errors of k_1 and k_2, respectively
σ_a', σ_b'	relative standard errors of a and b, respectively
$\sigma_{k1}', \sigma_{k1}'$	relative standard errors of k_1 and k_2, respectively
ϕ_s	local potential
η	overall overpotential
η_a	activation overpotential
η_c	concentration overpotential
η, η_G	cell efficiency
η_F	charge or Faradaic efficiency

[6] At the time the present paper is written out in full a current investigation on the relation between the state-of-charge, the cell capacity and the f_a factor are being carried out.

Mathematical expressions

ΔG	free energy change; potential barrier
ΔH	enthalpy energy change
Δm	change in mass during chemical reaction; change in density variation slope
Δt	time interval
$\Delta \rho$	density variation
$\Delta \Phi$	external potential difference
$\Delta \epsilon$	internal potential difference

References

[1] D. Pavlov, I. Balkanov, P. Rachev, *J. Electrochemical Soc., 134* (1987) 2390.

[2] P. Ruetschi, *J. of Power Sources, 2* (1977/78) 3.

[3] E.J. Euler, *Bull. Schweiz. Elektrotech. Ver., 61* (1970) 1054.

[4] E.J. Ritchie, *Trans. Electrochem. Soc., 92* (1947) 229.

[5] Th. J. Hughel and R.H. Hammer, in D.H. Collins (ed.), *Power Sources 3*, Oriel Press, Newcastle upon Tyne, 1971, p. 35.

[6] M.P.J. Brennan and N.A. Hampson, *J. Electroanal. Chem., 48* (1973) 465.

[7] E.G. Yampol'skaya, *Electrokhymia, 8* (1972) 1325.

[8] A. Simon, S.M. Caulder, P.J. Gurluski and J.R. Pierson, *J. Electrochem. Soc., 121* (1974) 463.

[9] G. Archdale and J.A. Harrison, *Electroanal. Chem., 34* (1972) 21; *39* (1972) 357; *43* (1973) 321; *47* (1973) 93.

[10] P. Ruetschi and B.D. Cahan, *J. Electrochem. Soc., 105* (1958) 369.

[11] D. Berndt and E. Voss, in D.H. Collins (ed.), *Batteries 2*, Pergamon Press, Oxford, 1965, p. 17.

[12] P. Ruetschi, J. Sklarchuck and R.T. Angstadt, *Electrochim. Acta, 8* (1963) 333.

[13] J. Doria, M.C. de Andrés, C. Armenta, J. Fullea and F. Graña, *J. Power Sources, 22* (1988) 115.

[14] D. Thuerk, *Proc. 30th Power Sources Conf.*, The Electrochemical Society, Pennington, NJ, USA, 1982, p. 89.

[15] K. Tomantschger, *J. Power Sources, 13* (1984) 137.

[16] J. Doria, M.C. de Andrés, C. Armenta, J. Fullea and F. Graña, *J. Power Sources, 27* (1989) 189.

[17] C. Armenta, *J. Power Sources, 27* (1989) 297.

[18] C. Armenta, J. Doria and M.C. de Andrés, *Solar Wind Technol., 7* (1990) 337.

[19] C. Armenta, J. Doria and M.C. de Andrés, *An. Física, B86* (1990) 50.